Z. angew. Math. Phys. 54 (2003) 1–30
0044-2275/03/050001-30
DOI 10.1007/s00033-003-1013-3

Zeitschrift für angewandte Mathematik und Physik ZAMP

Blow-up and pattern formation in hyperbolic models for chemotaxis in 1-D

T. Hillen and H. A. Levine *

This paper is dedicated to Larry Payne on the occasion of his 75^{th} birthday.

Abstract. In this paper we study finite time blow-up of solutions of a hyperbolic model for chemotaxis. Using appropriate scaling this hyperbolic model leads to a parabolic model as studied by Othmer and Stevens (1997) and Levine and Sleeman (1997). In the latter paper, explicit solutions which blow-up in finite time were constructed. Here, we adapt their method to construct a corresponding blow-up solution of the hyperbolic model. This construction enables us to compare the blow-up times of the corresponding models. We find that the hyperbolic blow-up is always later than the parabolic blow-up. Moreover, we show that solutions of the hyperbolic problem become negative near blow-up. We calculate the "zero-turning-rate" time explicitly and we show that this time can be either larger or smaller than the parabolic blow-up time.

The blow-up models as discussed here and elsewhere are limiting cases of more realistic models for chemotaxis. At the end of the paper we discuss the relevance to biology and exhibit numerical solutions of more realistic models.

Mathematics Subject Classification (2000).

Keywords.

1. Introduction

In this paper we investigate the qualitative behavior of solutions of the following hyperbolic model for chemotaxis in 1-D:

$$\begin{aligned} u_t^+ + \gamma u_x^+ &= -\mu^+(S,S_x)u^+ + \mu^-(S,S_x)u^- \\ u_t^- - \gamma u_x^- &= \mu^+(S,S_x)u^+ - \mu^-(S,S_x)u^- \\ S_t &= R(S,u^+ + u^-), \end{aligned} \tag{1}$$

Here $u^{\pm}(t,x)$ denote the particle densities of right $(+)$/left$(-)$ moving particles, γ denotes the mean particle speed, and $\mu^{\pm}(S,S_x)$ are turning rates (rates

* HL thanks The Max-Planck-Institut für Mathematik in den Naturwissenschaften its support during the preparation of this paper

of change of direction from + to − and vice versa). The turning rates depend not only on the concentration $S(t,x)$ of the chemical signal, but also on its spatial gradient, $S_x(t,x)$. In many examples of chemotactic behavior, such as for the slime mold *Dictyostelium discoideum* (Dd), the bacteria *Eschirichia coli* or *Salmonella typhimurium*, the external chemical signal S is produced or consumed by the cell species itself. This is modeled by the precise form of the reaction term $R(S, u^+ + u^-)$.

We consider the system (1) on an interval $I = [0, l]$ with homogeneous Neumann boundary conditions

$$u^+(t,0) = u^-(t,0), \qquad u^-(t,l) = u^+(t,l). \tag{2}$$

We study three different forms of turning rates, all of which appear in the literature

$$\mu_a^{\pm}(S, S_x) := \frac{\gamma}{2D}(\gamma \mp \chi(S)S_x) \tag{3}$$

$$\mu_b^{\pm}(S, S_x) := \frac{\gamma}{2D}(\gamma \mp \chi(S)S_x)_+ \tag{4}$$

$$\mu_c^{\pm}(S, S_x) := \frac{\gamma^2}{2D}\exp\left(\mp\frac{\chi(S)}{\gamma}S_x\right) \tag{5}$$

From experimental observations (see e.g. Rivero et al. [24] or Ford et al. [5]) the exponential dependence in μ_c is the most realistic model assumption. The form of μ_a is appropriate for shallow chemical gradients, or for small chemotactic sensitivities χ, or for large speed γ. However, in such cases, the turning rates μ_a can become negative. Hence we additionally impose a restriction as for μ_b. We call system (1) with (3) the *unrestricted problem*, system (1) with (4) the *restricted problem*, and system (1) with (5) the *exponential problem*.

We are interested in solutions which may blow up in finite time. As shown in Hillen and Stevens [10] for a similar model, finite time blow-up implies that $\|S(t,.)\|_{W^{1,\infty}}$ diverges to $+\infty$ in finite time. Hence μ_a, as approximation to μ_c is certainly not justified. On the other hand, in the scaling limit of γ, μ large the unrestricted system ((1) with (3)) converges to the original diffusion based model (6) below, discussed in Levine and Sleeman [17]. Hence the unrestricted problem appears as a generalization of (6).

We construct an exact solution for the unrestricted problem (when $\chi(S) = 1/S$) and thus obtain an explicit blow up time. We show that this blow up time is larger than the blow up time for the corresponding parabolic model. However, the turning rates vanish at points arbitrarily close to the blow up point before the solution blows up in finite time. We call the first time for which one of the turning rates vanish, the *zero-turning-rate time* and we find an explicit formula for it. As it should be, this time is always smaller than the blow up time. The positivity of the densities $u^{\pm}$ is no longer guaranteed. Indeed, we prove that these densities become negative close to the blow-up time. Negative densities are certainly uninteresting from a biological point of view. This means that the hyperbolic model becomes

invalid just before blow-up occurs. On the other hand, the cell densities remain positive at least until the turning rates become negative for the first time. We are able to show that under certain circumstances, the zero-turning rate time is larger than the blow-up time for the comparable diffusion based model. Thus the solution of the hyperbolic model remains positive and bounded for a short time after the blow-up of the solution of the parabolic model. This sheds new light on the meaning of "blow-up". Blow-up indicates that a particular model is no longer suitable to describe the biological phenomenon, it does not imply that blow-up should be observed in nature. The often used interpretation of fruiting bodies to correspond to blow-up solutions can not be true.

Negative turning rates can be interpreted as "alignment" terms. If there are many particles moving to the right, then they force left moving particles change direction and move to the right as well. This effect becomes so strong near blow up, that it leads to negative density for $u^{\pm}$. The random walk system (1) can be transformed into an equivalent system for the total particle density, $u = u^+ + u^-$, and the particle flux, $v = u^+ - u^-$. The resulting system for (u, v), (13) and (47), is known as Cattaneo system and it consists of a conservation law and a flux law (for Cattaneo systems for chemotaxis see [3]). Although $u^{\pm}$ become negative somewhere we show that the total particle density u remains positive everywhere.

F. Lutscher in [18] develops and studies one dimensional models for alignment, where positivity of the densities $u^{\pm}$ is preserved. Unfortunately, the model considered here, in case of negative turning rates, does not fall into the general framework of Lutscher.

Using a comparison argument we show in section 3.2 that solutions of the restricted problem exist as least as long as solutions for the unrestricted problem and that near blow-up the exponential problem grows faster. Finally we discuss the relation of the blow up result to more realistic scenarios and we show numerical simulations.

The remainder of this introduction is devoted to an explanation of the above model and to the choice of $\mu^{\pm}$ in both from a biological and from a theoretical point of view.

1.1. Diffusion based models for chemotaxis

Chemotaxis is the active orientation of moving organisms along chemical gradients. It is observed in many natural systems and has been studied in great detail for slime molds such as Dd [21] and bacteria, such as Salmonella typhimurium [26]. Chemotaxis plays a major role in tumor growth and angiogenesis. See [1, 2, 14, 16, 15, 13] and the references cited therein.

The phenomenon of chemotaxis and aggregation was studied mathematically beginning with the early papers of Patlak 1953 [23] and Keller and Segel 1970 [12]. The first result on finite time blow-up was obtained by Jäger and Luckhaus in 1992 [11]. Since then the mathematical literature on finite time blow-up for the Patlak-Keller-Segel model has grown rapidly. For a review of the recent literature, see Hillen [7]. Among all these results it is necessary to recall the results of [17] in some detail since the results presented here are directly related to some of those obtained there.

In [17] $P(t,x)$ and $W(t,x)$ denoted particle density and the chemical signal, respectively. The model in [17] reads

$$\begin{aligned} P_t &= D(P_x - P\chi(W)W_x)_x \\ W_t &= R(W,P), \end{aligned} \tag{6}$$

where D is the diffusion constant and $\chi(W)$ is the chemotactic sensitivity. The production-consumption function $R(W,P)$ is the same as for (1). Model (6) was based on modeling considerations discussed in [22]. There it was suggested that the above system might show finite time blow-up for the choice of $\chi(W) = \frac{1}{W}$ and $R(W,P) = WP$. This was supported by numerical simulations in [22]. In [17] an explicit solution was found which indeed blows up in finite time. On the interval $I = [0,\pi]$ the initial conditions for this explicit solution are:

$$\begin{aligned} P(x,0) &= \frac{1 + 2\varepsilon(1 - N\bar{c}_{\text{LS}})\cos(Nx) + (1 - N\bar{c}_{\text{LS}})\varepsilon^2}{1 + 2\varepsilon\cos(Nx) + \varepsilon^2} \qquad (7) \\ &\approx 1 - 2\varepsilon N\bar{c}_{\text{LS}}\cos(Nx), \\ W(x,0) &= \frac{1}{1 + 2\varepsilon\cos(Nx) + \varepsilon^2}, \qquad (8) \\ &\approx 1 - 2\varepsilon\cos(Nx) \end{aligned}$$

for $0 < \varepsilon < 1$, $N \in \mathbb{N}$, where $\bar{c}_{\text{LS}}$ is the positive root of

$$\bar{q}_{\text{LS}}(c) = c^2 + Nc - 1 = 0. \tag{9}$$

The blow-up time is then

$$T(\varepsilon, N) = \frac{-\ln|\varepsilon|}{N\bar{c}_{\text{LS}}}. \tag{10}$$

Let ℓ be a nonnegative integer. For $1 > \varepsilon > 0$, single point blow up occurs at points $x_\ell = (2\ell+1)/N$ in $[0,\pi]$. When $0 > \varepsilon > -1$, the blow up points are $x_\ell = 2\ell/N$ in $[0,\pi]$. Thus, if $N = 2$, the blow up point will occur at $x = \pi/2$ if and only if $1 > \epsilon > 0$. A calculation shows that $1 > N\bar{c}_{\text{LS}} > 2/(1+\sqrt{5})$.

The solution has the form

$$W(x,t) = \exp(\Psi(x,t)) \qquad \text{and} \qquad P(x,t) = \Psi_t(x,t),$$

where the auxiliary function $\Psi(x,t)$ is given by

$$\Psi(x,t) = t - \ln[1 + 2\varepsilon e^{N\bar{c}_{\text{LS}}t}\cos(Nx) + \varepsilon^2 e^{2N\bar{c}_{\text{LS}}t}]. \tag{11}$$

Remark 1.1. The meaning of the solution is the following: The vector $[P_0(x,t), W_0(x,t)]^t \equiv [1, e^t]^t$ is a spatially homogeneous solution of (6) with $[1,1]$ as initial data. Given any mode number N, there is a direction $[P_N, W_N]^t \equiv [N\bar{c}_{\text{LS}}, 1]^t\cos(Nx)$ in the closed subspace of $L^2(0,\pi)\times L^2(0,\pi)$ consisting of the closure of functions which satisfy $P[\log(P/W)]_x = 0$ at $x = 0, \pi$, and a curve given by $\overrightarrow{R}(\varepsilon) \equiv [P(\cdot,0,\varepsilon), W(\cdot,0,\varepsilon)]^t$ in $L^2(0,\pi)\times L^2(0,\pi)$ of initial data passing through $[1,1]$ with the property that any solution initially emanating from this curve will blow up in a finite time.

(This interpretation was not spelled out in [17].) The result tells us that in every neighborhood of the initial data for the spatially homogeneous solution $[1, e^t]^t$, there are solutions of arbitrarily high mode number which begin in this neighborhood and blow up in finite time. The numerical evidence suggests, but does not prove, that every arbitrarily small non constant perturbation of the initial data for $[1, e^t]^t$ (which must have a non trivial projection onto at least one of the directions $[N\bar{c}_{\text{LS}}, 1]^t\cos(Nx)$ for some N) must blow up in finite time.

1.2. Hyperbolic models for chemotaxis

There are several reasons to study hyperbolic models for chemotaxis as extensions of diffusion based models. For example, as one sees from the representation formula for the solution of the initial value problem for the heat equation, $u(\cdot,t) = G * u_0(t)$, solutions for which the initial function u_0 has compact support become everywhere positive for arbitrarily small $t > 0$, i.e., the propagation speed for such classical diffusion based models is infinite. Einstein [4] criticized such diffusion based models in 1906 as being physically unrealistic for small times.

The underlying model assumptions and parameters which lead to hyperbolic models on the one hand and to parabolic models on the other hand are very different. The parameters for diffusion based models, such as diffusion rate D or drift coefficients, e.g. $\chi(S)$, are related to *population* spread. They are measured in experiments by mean squared displacements or mean drifts of the population as a whole. Hyperbolic models, in contrast, are based on the *individual* movement properties of the species at hand, such as the speed γ and turning rates $\mu^{\pm}$. These are measured by following individual particles and evaluating its path. From this point of view, one can view hyperbolic models as based on the movements of individuals while parabolic models are based on the ensemble average movement of populations as a whole.

Segel, in [25], first used the hyperbolic model (1) to analyze a very specific scenario. Later Rivero *et al* [24] and Ford *et al* [6, 5] used it to describe experimental data. Hillen and Stevens [10] and Hillen, Rohde, Lutscher [9] studied the

hyperbolic chemotaxis model in 1-D from a more theoretical perspective. In these works, the issues of local and global in time existence of solutions were considered theoretically and numerically. The present work is in fact a continuation of the two previous papers [9, **?**]. In more than one space dimension Hillen and Othmer [8, 20] considered transport models while in [3], the authors studied Cattaneo-type models. An extensive review can be found in [7].

Diffusion based models can be considered to be the *parabolic limit* of hyperbolic models. This limit appears either for large speed and large turning rate or for appropriately scaled time and space variables. In the latter case the diffusion based models are the outer expansions of a singular perturbation expansion of the hyperbolic model [8, 20].

In case of large speeds and turning rates the quotient $\frac{\gamma^2}{\mu^+ + \mu^-}$ plays the role of an *effective diffusion coefficient*. For each of the turning rates μ_a, μ_b and μ_c as defined above (3)-(5), we can define a corresponding effective diffusion coefficient

$$D_j(\gamma) := \frac{\gamma^2}{\mu_j^+ + \mu_j^-}, \qquad \text{for} \quad j \in \{a, b, c\}.$$

We see that in each case $D_j(\gamma) \to D$ as $\gamma \to \infty$.

2. The unrestricted problem

Here the hyperbolic chemotaxis model (1) with Neumann boundary conditions (2) with the choice of $\mu^\pm$ as in (3), $\chi(S) = \frac{a}{S}$ and $R(S, u^+ + u^-) = S(u^+ + u^-)$ is investigated.

By a local solution of (1) with Neumann boundary conditions (2) we mean a classical solution on some space-time cylinder $[0, \pi] \times [0, T_{exist})$. A local solution is said to be global if $T_{exist} = +\infty$.

The following theorem is established:

Theorem 2.1. *For the above choices of χ, R, in every neighborhood of the initial data for the spatially homogeneous solution $(U^+, U^-, S) = (1/2, 1/2, e^t)$, there is a solution with data in this neighborhood which blows up in finite time.*

Proof. To prove this, we construct a solution with data in a uniform neighborhood of $(1/2, 1/2, 1)$ which blows up in finite time. Following the methods developed in [17], the above system is reduced to a single higher order equation for a single function Ψ. Then a series solution ansatz is used to find an explicit solution which blows up in finite time.

In the case studied here we have

$$\mu_a^\pm(S, S_x) = \frac{\gamma}{2D}(\gamma \mp \chi(S)S_x). \tag{12}$$

We rewrite system (1) as a system for $u = u^+ + u^-$ and $v = u^+ - u^-$:

$$\begin{aligned} u_t + \gamma v_x &= 0, \\ v_t + \gamma u_x &= \frac{a\gamma}{D}\frac{uS_x}{S} - \frac{\gamma^2}{D}v, \\ S_t &= Su. \end{aligned} \tag{13}$$

Now define

$$\Psi(t,x) := \ln\left(S(t,x)\right),$$

a definition that is meaningful in view of the physical interpretation of S as a concentration.† It follows that

$$\Psi_t = \frac{S_t}{S} = u \qquad \text{and} \qquad \Psi_x = \frac{S_x}{S}.$$

The first equation in (13) can be written as

$$\Psi_{tt} + \gamma v_x = 0, \tag{14}$$

while the second equation of (13) reads

$$v_t + \gamma \Psi_{tx} = \frac{\gamma}{D}\left(-\gamma v + a\Psi_t\Psi_x\right). \tag{15}$$

Differentiating both sides of (14) with respect to t, both sides of (15) with respect to x and eliminating v_{tx} between the resulting equations leads to

$$D\Psi_{txx} - \frac{D}{\gamma^2}\Psi_{ttt} = \Psi_{tt} + a\left(\Psi_t\Psi_x\right)_x. \tag{16}$$

As in [17] set

$$\Psi = t + h.$$

Then for $a = 1$ (which corresponds to $a = -1$ in [17]),

$$Dh_{txx} - \frac{D}{\gamma^2}h_{ttt} = h_{tt} + h_{xx} + (h_x h_t)_x. \tag{17}$$

To compare this equation with the corresponding equation considered in [17], which did not include the term h_{ttt}, let $D = 1$ and keep γ as a free parameter. Later we will see how γ modifies the blow-up time. We write (17) in the following form:

$$h_{tt} + h_{xx} - h_{txx} = -\frac{1}{\gamma^2}h_{ttt} - (h_x h_t)_x \tag{18}$$

† The meaning of $-\psi$ as the negative logarithm of concentration is the same as that of pH for aqueous solutions, i. e., the negative (base 10) logarithm of the hydrogen ion concentration. The equation $-\psi_t = u$ is just the statement that the cell density increases linearly with the rate of change of pS.

In the parabolic limit for $\gamma \to \infty$ the h_{ttt} term vanishes and equation (3.2a) of [17] results. As in [17], choose $l = \pi$ and assume a solution of series-form

$$h(t,x) = \sum_{n=1}^{\infty} a_n e^{Nnct} \cos(Nnx). \tag{19}$$

This function corresponds to the ansatz chosen in [17], where $N \in \mathbb{N}$ specifies the number of inner local maxima. The case $N = 2$ leads to solutions which have a single maximum or minimum in the center of the domain. For the above choice of $h(t,x)$ in (19)

$$\begin{aligned} h_{tt} &= \sum_{n=1}^{\infty} N^2 c^2 n^2 a_n e^{Nnct} \cos(Nnx) \\ h_{xx} &= \sum_{n=1}^{\infty} -N^2 n^2 a_n e^{Nnct} \cos(Nnx) \\ h_{txx} &= \sum_{n=1}^{\infty} -N^3 n^3 c a_n e^{Nnct} \cos(Nnx) \\ h_{ttt} &= \sum_{n=1}^{\infty} N^3 n^3 c^3 a_n e^{Nnct} \cos(Nnx) \end{aligned}$$

and as shown in [17], using the addition formulas for sin and cos :

$$(h_x h_t)_x = -\frac{1}{2} N^3 c \sum_{n=1}^{\infty} n \left(\sum_{k=1}^{n} k(n-k) a_k a_{n-k} \right) e^{Nnct} \cos(Nnx).$$

Then the left hand side of (18) becomes

$$h_{tt} + h_{xx} - h_{txx} = \sum_{n=1}^{\infty} N^2 n^2 (c^2 - 1 + Nnc) a_n e^{Nnct} \cos(Nnx)$$

while the right hand side of (18) may be written as

$$\begin{aligned} &-\frac{1}{\gamma^2} h_{ttt} - (h_x h_t)_x \\ &\quad = \sum_{n=1}^{\infty} \left(\frac{-N^3 n^3 c^3}{\gamma^2} a_n + \frac{1}{2} N^3 nc \sum_{k=1}^{n} k(n-k) a_k a_{n-k} e^{Nnct} \cos(Nnx) \right). \end{aligned} \tag{20}$$

Comparing coefficients, it follows that for each $n \geq 1$:

$$\left(N^2 n^2 (c^2 - 1) + N^3 n^3 c + \frac{N^3 n^3 c^3}{\gamma^2} \right) a_n = \frac{1}{2} N^3 nc \sum_{k=1}^{n} k(n-k) a_k a_{n-k}.$$

In particular for $n = 1$

$$\left(N^2 (c^2 - 1) + N^3 c + \frac{N^3 c^3}{\gamma^2} \right) a_1 = 0.$$

For the cubic

$$q(c) = \frac{N}{\gamma^2}c^3 + c^2 + Nc - 1, \tag{21}$$

notice that $q(0) = -1$, $q(1/2) = \frac{N}{8\gamma^2} + \frac{N}{2} - \frac{3}{4} > 0$, for $N \geq 2$, and $q'(c) = \frac{3N}{\gamma^2}c^2 + 2c + N$ which is positive for $c > 0$. Thus this cubic has a unique positive root, $\bar{c}$ say, which must satisfy $\bar{c} \in (0, 1/2)$. † For $c = \bar{c}$ one can choose a_1 arbitrarily.

For $n > 1$ we get from (20)

$$\left(\frac{Nn}{\gamma^2}\,\bar{c}^3 + \bar{c}^2 - 1 + Nn\bar{c}\right) na_n = \frac{1}{2}N\bar{c}\sum_{k=1}^{n-1} ka_k(n-k)a_{n-k}$$

which may be simplified by defining $b_n \equiv na_n$ to obtain

$$\left(\frac{Nn}{\gamma^2}\,\bar{c}^3 + \bar{c}^2 - 1 + Nn\bar{c}\right) b_n = \frac{1}{2}N\bar{c}\sum_{k=1}^{n-1} b_k b_{n-k}. \tag{22}$$

If $\bar{c}$ is any root of $q(c) = 0$ with q given in (21), then $\frac{N}{\gamma^2}\,\bar{c}^3 + N\bar{c} = 1 - \bar{c}^2$. Notice also that $q(-1) = -\frac{N}{\gamma^2} - N \neq 0$, so that no root of $q(c)$ is a root of unity. This simplifies the left hand side of (22) so that

$$\left(\frac{Nn}{\gamma^2}\,\bar{c}^3 + \bar{c}^2 - 1 + Nn\bar{c}\right) = (n-1)(1-\bar{c}^2).$$

From (22) it follows that

$$b_n = \frac{N\bar{c}}{2(n-1)(1-\bar{c}^2)}\sum_{k=1}^{n-1} b_k b_{n-k}. \tag{23}$$

Equation (23) simplifies further if one takes b_n in the form

$$b_n = \frac{2(1-\bar{c}^2)}{N\bar{c}}\varepsilon_n$$

where ε_n will be chosen later. For this choice of b_n, from (23) we obtain

$$\frac{2(1-\bar{c}^2)}{N\bar{c}}\varepsilon_n = \frac{1}{n-1}\,\frac{N\bar{c}}{2(1-\bar{c}^2)}\sum_{k=1}^{n-1}\left(\frac{2(1-\bar{c}^2)}{N\bar{c}}\right)^2 \varepsilon_k\varepsilon_{n-k}$$

† This cubic has no negative roots if the discriminant of the quadratic $q'(c)$ is negative, i. e. in case of N=2, if $\gamma^2 < 12$. If this inequality fails it will have zero, one or two roots according as $q(c_-) < 0$, $q(c_-) = 0$ or $q(c_-) > 0$ where c_- is the smaller of the two (necessarily negative) roots of $q'(c) = 0$. The corresponding solutions will not be seen in computations made based on finite difference or finite element calculations as they will be dominated by the components of the numerical solution in the direction of the solution corresponding to the positive root.

Thus

$$\varepsilon_n = \frac{1}{n-1}\sum_{k=1}^{n-1}\varepsilon_k\varepsilon_{n-k}. \tag{24}$$

Finally, if $\varepsilon_1 = \varepsilon$, it follows from equation (24) that $\varepsilon_2 = \varepsilon^2$. By an induction argument, $\varepsilon_n = \varepsilon^n$.
Therefore

$$a_n = \frac{1}{n}b_n = \frac{2(1-\bar{c}^2)}{N\bar{c}}\ \frac{\varepsilon^n}{n}.$$

Hence a candidate for a solution of (18) is

$$h(t,x) = \frac{2(1-\bar{c}^2)}{N\bar{c}}\sum_{n=1}^{\infty}\frac{\varepsilon^n}{n}e^{Nn\bar{c}t}\cos(Nnx) \tag{25}$$

By the ratio test, the sum in (25) converges absolutely and uniformly if and only if

$$|\varepsilon|e^{N\bar{c}t} = \lim_{n\to\infty}\left|\frac{\varepsilon^{n+1}}{n+1}e^{N(n+1)\bar{c}t}\frac{n}{\varepsilon^n}e^{-Nn\bar{c}t}\right| < 1. \tag{26}$$

If $\bar{c} < 0$, this is true for any $\varepsilon \in (-1,1)$ Thus, whenever $q(c)$ has negative roots, the solutions given by (25) with $\varepsilon \in (-1,1)$ are stable, and in fact, converge uniformly to zero, i.e., Ψ converges uniformly to $\Psi = t$.

Next suppose $\bar{c} > 0$ and $\varepsilon \in (-1,1)$. The first time such that (26) is violated occurs when

$$t = T_h = \frac{-\ln|\varepsilon|}{N\bar{c}}. \tag{27}$$

This T_h is the blow-up time of the solution of our hyperbolic model given in (25). For $N = 2$ and $\varepsilon > 0$, the single blow up point is $(\frac{\pi}{2}, T_h)$.

Just as in [17], by writing $\cos\theta = (\exp(i\theta) + \exp(-i\theta))/2$ one can sum the resulting geometric series in (25) to find that (after replacing ε by $-\varepsilon$ to set the blow up point in the center of the interval for positive ε):

$$\Psi(x,t) = t - \ln(1 + 2\varepsilon e^{N\bar{c}t}\cos(Nx) + \varepsilon^2 e^{2N\bar{c}t}). \tag{28}$$

Then

$$S(x,t) = \exp(\Psi(x,t)), \qquad u(x,t) = \Psi_t(x,t).$$

The function $v(x,t)$ is found from the second equation of (13) to be

$$v(x,t) = v(x,0)e^{-\gamma^2 t} + \int_0^t [a\Psi_x(x,s) - \gamma\Psi_s(x,s)]e^{\gamma^2(s-t)}\,ds. \tag{29}$$

The function $v(x,0)$ is the initial difference between the densities of the right and left moving particles. Without loss, one may assume at the outset that $v(x,0) = 0$.

The initial conditions for this particular solution are

$$\begin{aligned} u(x,0) &= \frac{1+2\varepsilon(1-N\bar{c})\cos(Nx)+(1-2N\bar{c})\varepsilon^2}{1+2\varepsilon\cos(2x)+\varepsilon^2}, \\ \Psi(x,0) &= -\ln(1+2\varepsilon\cos(Nx)+\varepsilon^2). \end{aligned} \tag{30}$$

The total mass of the exact solution is given by

$$U_0(\varepsilon) = \int_0^{2\pi} u(x,0)\,dx.$$

Then $u^{\pm}(x,0) = (1/2)u(x,0)$. It is easy to check that as $\varepsilon \to 0$,

$$(u^+(x,0), u^-(x,0), S(x,0)) \to (1/2, 1/2, 1)$$

uniformly in x which is the initial data for the spatially homogeneous solution $(U^+, U^-, S) = (1/2, 1/2, e^t)$ as was claimed.

□

Next, notice that

$$\Psi_x(x,0) = \frac{2N\varepsilon\sin(Nx)}{1+2\varepsilon\cos(Nx)+\varepsilon^2}$$

so that for small enough ε, the turning rates are initially positive. Therefore the solution is local in the above sense.

At the blow up time for $x \neq \pi/2$,

$$\mu^{\pm} = \frac{\gamma}{2}[\gamma \mp \Psi_x] = \gamma\left[\frac{\gamma}{2} \mp \tan\left(\frac{Nx}{2}\right)\right].$$

Thus the turning rates for this solution must change sign at some time earlier than the blow up time.

Remark 2.2. The geometric interpretation of the resulting solution is precisely the same as that discussed in Remark 1.1.

The turning rates change sign near the center of the interval where u is blowing up. Notice that μ^+ vanishes at a point to the left of $\pi/2$ while the same is true for μ^- to the right of $\pi/2$. In other words, to the left of the center point, particles that are moving to the left are being converted to particles that are moving to the right while to the right of the center point, the reverse is true.

In Hillen and Stevens [10] it was shown that if the turning rates are positive and the initial populations are positive, then the solutions stay positive for all times in the existence interval. We will show later that in the case studied here the negative turning rates will ultimately lead to densities $u^{\pm}$ which become negative near the blow-up point. First we study the *zero-turning-rate time*.

2.1. The zero-turning-rate time

By the choice of the turning rates (3) we find that one of the turning rates becomes zero as soon as the *eikonal equation*

$$|\Psi_x(x, T(x))| = \gamma \tag{31}$$

is satisfied for some $x \in [0, \pi]$. We denote with T_{tr} the first time such that (31) is satisfied for some $x \in [0, \pi]$. For $N = 2$ we give an explicit formula for T_{tr} in (32).

Since $T_{tr}(x)$ is to be a minimum at some point $x = x_1$ in $(0, \pi)$ † and since Ψ_x is analytic except at the blow up point, it must be the case that $T'_{tr}(x_1) = 0$. By the implicit function theorem, in the case $\Psi_x > 0$,

$$\Psi_x(x_1, T_{tr}(x_1)) = \gamma$$

and

$$0 = \Psi_{xx}(x_1, T_{tr}(x_1)) + \Psi_{xt}(x_1, T_{tr}(x_1))T'_{tr}(x_1) = \Psi_{xx}(x_1, T_{tr}(x_1)).$$

Setting $Z = \varepsilon \exp[2\bar{c}T_{tr}(x_1)]$, these equations yield:

$$\begin{aligned} \gamma &= \frac{4Z\sin(2x_1)}{1 + 2Z\cos(2x_1) + Z^2}, \\ 8Z\cos(2x_1) &= \frac{-(4Z\sin(2x_1))^2}{1 + 2Z\cos(2x_1) + Z^2}. \end{aligned}$$

From these, $\tan(2x_1) = -2/\gamma$, an equation which has one root in $(\pi/4, \pi/2)$ and one in $(3\pi/4, \pi)$. Since the preceding equations tell us that the sine must be positive and the cosine negative, we have

$$\cos(2x_1) = \frac{-\gamma}{\sqrt{4 + \gamma^2}}, \quad \sin(2x_1) = \frac{2}{\sqrt{4 + \gamma^2}}$$

and $x \in (\pi/4, \pi/2)$. This leads to the quadratic

$$0 = \gamma(1 + Z^2) - 2\sqrt{4 + \gamma^2}Z.$$

Solving the quadratic and taking the smaller root (the only root in $(0, 1)$) one finds that the turning rate first changes sign at time

$$T_{tr} = -\frac{\ln \varepsilon}{2\bar{c}} + \frac{\ln Z(\gamma)}{2\bar{c}} \tag{32}$$

where

$$Z(\gamma) = \frac{\gamma/2}{\sqrt{1 + (\gamma/2)^2} + 1.} \tag{33}$$

The corresponding blow up time for the unrestricted hyperbolic problem is

$$T_h = \frac{-\ln \varepsilon}{2\bar{c}}.$$

† If $\gamma > 0$, x_1 cannot be an end point.

As remarked above, the turning rates vanish before the solution of the unrestricted hyperbolic problem blows up (if it does at all) and indeed $0 < T_{tr} < T_h$. Notice that $T_{tr}/T_h - 1 \to 0$ as $\gamma \to +\infty$.

Notice also that if $\varepsilon > Z(\gamma)$, the solution fails to be local in the sense of the definition if it is started at time zero. If the solution is started at a time $\bar{t} < T_{tr}$, then the solution will be local on $[\bar{t}, T_{tr}]$. As $\gamma \to 0$, $\bar{t} \to -\infty$.

2.2. Negative densities $u^{\pm}$ near blow up

Since the turning rates become negative near blow-up, we can no longer guarantee that the densities $u^{\pm}$ stay non-negative. Indeed, for $N = 2$ and $\varepsilon > 0$ we prove that if γ is small enough and t close to T_h, then in a neighborhood of the blow-up point $x = \pi/2$ there is an interval to the right of $\pi/2$ where $u^+(x,t) < 0$, and another interval to the left of $\pi/2$ where $u^-(x,t) < 0$. Close to $\pi/2$ we find always $u^{\pm}(x,t) > 0$ and in the whole neighborhood we have always $u(x,t) > 0$.

Theorem 2.3. *Let $\alpha \in (T_{tr}/T_h, 1)$. There exist $\gamma^*(\alpha) > 0$ such that for each $\gamma < \gamma^*$ there exists $t^*(\gamma)$ and $\delta, \rho, \kappa > 0$ with $\delta > \rho > \kappa$ such that for all t with $T_{tr} \le t^* \le t \le \alpha T_h$*

$$\begin{aligned}
&(\mathbf{i}) && u^+(x,t) < 0, \quad \textit{for} \quad x \in \left(\frac{\pi}{2} + \rho, \frac{\pi}{2} + \delta\right)\\
&(\mathbf{ii}) && u^-(x,t) < 0, \quad \textit{for} \quad x \in \left(\frac{\pi}{2} - \delta, \frac{\pi}{2} - \rho\right)\\
&(\mathbf{iii}) && u^+(x,t) > 0, \quad \textit{for} \quad x \in \left(\frac{\pi}{2} - \delta, \frac{\pi}{2} + \kappa\right)\\
&(\mathbf{iv}) && u^-(x,t) > 0, \quad \textit{for} \quad x \in \left(\frac{\pi}{2} - \kappa, \frac{\pi}{2} + \delta\right)
\end{aligned}$$

Moreover we have for all t with $T_{tr} \le t \le \alpha T_h$ that

$$(\mathbf{v}) \qquad u(x,t) > 0, \quad \textit{for} \quad x \in \left(\frac{\pi}{2} - \delta, \frac{\pi}{2} + \delta\right).$$

Proof. We use asymptotic arguments near the blow up point to prove this result. In (29) we see that $v(x,t)$ can be expressed in terms of derivatives of $\Psi(x,t)$, which is given in (28). For $N = 2$ and $\varepsilon > 0$ we summarize:

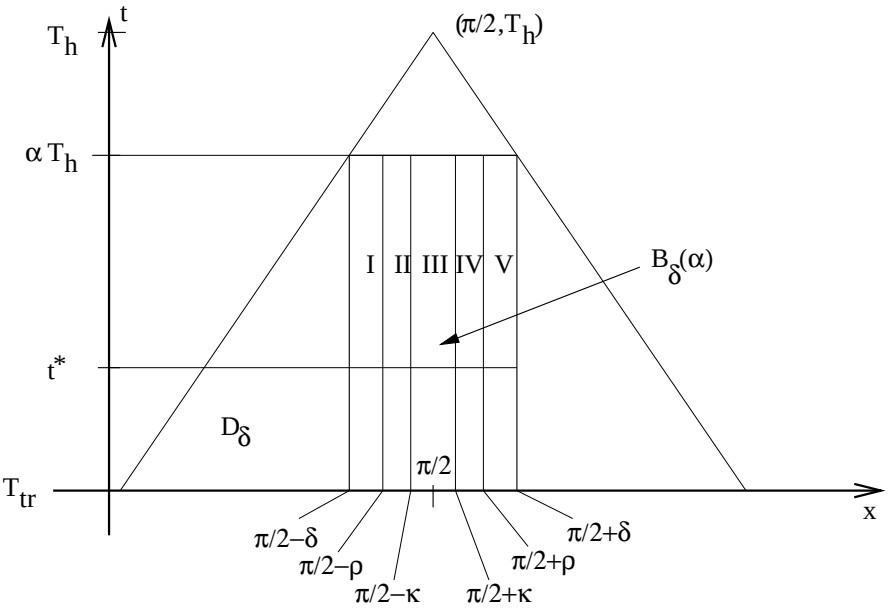

Figure 1. Schematic of the proof of Theorem 2.3. Inside the cone D_δ we find a cylinder $B_\delta(\alpha)$ which for $t^* < t \le \alpha T_h$ is divided into five subregions. We show that $u^- < 0$ on I, $u^- > 0$ on $III \cup IV \cup V$, $u^+ < 0$ on V, $u^+ > 0$ on $I \cup II \cup III$, and $u = u^+ + u^- > 0$ on $I \cup II \cup III \cup IV \cup V$.

Lemma 2.4.

$$\begin{aligned}
\Psi(x,t) &= t - \ln\left(1 + 2\varepsilon e^{2\bar{c}t}\cos(2x) + \varepsilon^2 e^{4\bar{c}t}\right),\\
\Psi_t(x,t) &= 1 - \frac{4\varepsilon\bar{c}e^{2\bar{c}t}\left(\cos(2x) + \varepsilon e^{2\bar{c}t}\right)}{1 + 2\varepsilon e^{2\bar{c}t}\cos(2x) + \varepsilon^2 e^{4\bar{c}t}},\\
\Psi_x(x,t) &= \frac{4\varepsilon e^{2\bar{c}t}\sin(2x)}{1 + 2\varepsilon e^{2\bar{c}t}\cos(2x) + \varepsilon^2 e^{4\bar{c}t}},\\
\Psi_{tx}(x,t) &= \frac{8\varepsilon\bar{c}e^{2\bar{c}t}\sin(2x)\left(1 - \varepsilon^2 e^{4\bar{c}t}\right)}{\left(1 + 2\varepsilon e^{2\bar{c}t}\cos(2x) + \varepsilon^2 e^{4\bar{c}t}\right)^2}.
\end{aligned}$$

Moreover

$$\Psi_t\Psi_x - \Psi_{xt} = (1 - 2\bar{c})\Psi_x. \tag{34}$$

Notice that

$$\begin{aligned}
\Psi(x,t) &= t - 2\ln\left(1 - \varepsilon e^{2\bar{c}t}\right) - 2\ln\left(1 + (\cos(2x)+1)/(\varepsilon e^{2\bar{c}t} - 1)^2\right)\\
&= t - 2\ln\left(1 - \varepsilon e^{2\bar{c}t}\right) - 2\ln\left(1 + (\cos(2x)+1)/(e^{2\bar{c}(T_h - t)} - 1)^2\right)
\end{aligned} \tag{35}$$

We illustrate the construction of the proof in Figure 1. Let $0 < \delta < (1-\alpha)\bar{c}T_h$

be fixed and let D_δ be a backward cone of points through $(\pi/2, T_h)$ defined as

$$D_\delta := \left\{ (x,t) : \left| x - \frac{\pi}{2} \right| \le \delta \frac{T_h - t}{T_h - \alpha T_h},\ T_{tr} \le t \le T_h \right\}$$

For each $\alpha \in (T_{tr}/T_h, 1)$ we consider a cylinder of width δ and height αT_h which is contained in D_δ:

$$B_\delta(\alpha) = \left\{ (x,t) : \left| x - \frac{\pi}{2} \right| \le \delta,\ T_{tr} \le t \le \alpha T_h \right\}$$

Notice that the logarithmic term in the second equation of (35) can be expanded in a power series in the variable $z \equiv (x - \frac{\pi}{2})/(\bar{c}(T_h - t))$. The convergence will be absolute and uniform as long as $|z| \le \delta/((1-\alpha)\bar{c}T_h) < 1$.

We have the following Lemma:

Lemma 2.5. *The expansions*

$$\begin{aligned}
\Psi(x,t) &= t - 2\ln\left(1 - \varepsilon e^{2\bar{c}t}\right) + \mathcal{O}\left(\left(x - \frac{\pi}{2}\right)^2\right) \\
u(x,t) = \Psi_t(x,t) &= 1 + \frac{4\varepsilon\bar{c}e^{2\bar{c}t}}{1 - \varepsilon e^{2\bar{c}t}} + \mathcal{O}\left(\left(x - \frac{\pi}{2}\right)^2\right) \\
\frac{S_x(x,t)}{S(x,t)} = \Psi_x(x,t) &= \frac{-8\varepsilon e^{2\bar{c}t}}{\left(1 - \varepsilon e^{2\bar{c}t}\right)^2}\left(x - \frac{\pi}{2}\right) + \mathcal{O}\left(\left(x - \frac{\pi}{2}\right)^2\right) \\
u_x(x,t) = \Psi_{tx}(x,t) &= \frac{-16\varepsilon\bar{c}e^{2\bar{c}t}\left(1 + \varepsilon e^{2\bar{c}t}\right)}{\left(1 - \varepsilon e^{2\bar{c}t}\right)^3}\left(x - \frac{\pi}{2}\right) + \mathcal{O}\left(\left(x - \frac{\pi}{2}\right)^2\right)
\end{aligned}$$

are valid on the set D_δ. On the set $B_\delta(\alpha)$ (where $T_h - t \ge (1-\alpha)T_h$ so that $|x - \pi/2| \le \delta \le \delta(T_h - t)/((1-\alpha)T_h)$), each order constant is proportional to some positive power of δ.

These expansions near $x = \pi/2$ reveal the nature of singularity which triggers the blow-up of these specific terms. For brevity, we write, to first order in $x - \pi/2$,

$$\Psi \approx \Theta_1(t), \quad \Psi_t \approx \Theta_2(t), \quad \Psi_x \approx \left(\frac{\pi}{2} - x\right)\Theta_3(t), \quad \Psi_{xt} \approx \left(\frac{\pi}{2} - x\right)\Theta_4(t),$$

with non-negative functions $\Theta_1(t), \ldots, \Theta_4(t)$, which can be easily identified from the above Lemma. With use of formula (34) we find that

$$\Psi_t\Psi_x - \Psi_{xt} = \left(\frac{\pi}{2} - x\right)(1 - 2\bar{c})\Theta_3(t) + \mathcal{O}\left(\left(x - \frac{\pi}{2}\right)^2\right).$$

With use of (29) we can then write $v(x,t)$ near $\pi/2$ as

$$v(x,t) = \gamma \int_0^t e^{\gamma^2(s-t)}(1 - 2\bar{c})\frac{8\varepsilon e^{2\bar{c}s}}{\left(1 - \varepsilon e^{2\bar{c}s}\right)^2} ds \left(\frac{\pi}{2} - x\right) + \mathcal{O}\left(\left(x - \frac{\pi}{2}\right)^2\right).$$

Now suppose $x > \pi/2$ and $t \le \alpha T_h$. Then we can choose δ small enough to ensure that the second order term can be neglected for $|x-\pi/2| \le \delta$. Notice that δ does not depend on γ. Then there is an interval

$$I_1 := \left(\frac{\pi}{2}+\rho, \frac{\pi}{2}+\delta\right)$$

such that $v(x,t) < 0$ on that interval as long as $t \le \alpha T_h$.

Using the inequalities $1 > e^{\gamma^2(s-t)} > e^{-\gamma^2 t}$ we estimate v from above and below:

$$0 > 4\gamma\frac{\varepsilon(1-2\bar{c})}{\bar{c}(1-\varepsilon)}\left(\frac{\pi}{2}-x\right)e^{-\gamma^2 t}\frac{(e^{2\bar{c}t}-1)}{1-\varepsilon e^{2\bar{c}t}} \ge v(x,t) \ge 4\gamma\frac{\varepsilon(1-2\bar{c})}{\bar{c}(1-\varepsilon)}\left(\frac{\pi}{2}-x\right)\frac{e^{2\bar{c}t}-1}{1-\varepsilon e^{2\bar{c}t}}. \tag{36}$$

Now consider $u^+ = (u+v)/2$ on this interval I_1. Since $v(x,t) < 0$ on I_1 we use estimate (36) to find that

$$u^+(x,t) \le 1 + \left[4\bar{c} + \left(\frac{\pi}{2}-x\right)2\gamma\frac{1-2\bar{c}}{\bar{c}}e^{-\gamma^2 t}\right]\frac{\varepsilon e^{2\bar{c}t}}{1-\varepsilon e^{2\bar{c}t}}. \tag{37}$$

(Here we are assuming that $\alpha T_h > t > \ln 2/(2\bar{c})$ so that $e^{2\bar{c}t}-1 \ge e^{2\bar{c}t}/2$.) We have also used $1-\varepsilon \approx 1$.)

We multiply the expression in the brackets by $\bar{c}/4$ and study the sign of

$$\bar{c}^2 + \frac{\gamma}{2}\left(\frac{\pi}{2}-x\right)(1-2\bar{c})e^{-\gamma^2 t}.$$

We claim that $\bar{c}(\gamma) \to 0$ as $\gamma \to 0$. We must choose γ small enough such that the second term dominates $\bar{c}^2$ on I_1. On I_1, $\pi/2 - x \le -\rho$. Hence it is sufficient to show that

$$\bar{c}^2 - \frac{\gamma}{2}\rho(1-2\bar{c})e^{-\gamma^2 t} < 0 \tag{38}$$

for appropriate $\gamma > 0$. Since $\bar{c}$ satisfies $q(\bar{c}) = 0$, where q is given in (21), we have

$$1 - 2\bar{c} = \bar{c}^2\left(\frac{2\bar{c}}{\gamma^2}+1\right)$$

Then (38) holds if

$$-\vartheta := \bar{c}^2\left(1 - \rho e^{-\gamma^2 t}\left(\frac{2\bar{c}}{\gamma}+\gamma\right)\right) < 0,$$

i.e., if

$$\rho e^{-\gamma^2 t}\left(\frac{2\bar{c}}{\gamma}+\gamma\right) > 1. \tag{39}$$

We have the following lemma:

Lemma 2.6. *The function $\gamma \mapsto \bar{c}(\gamma)/\gamma$ is monotonically decreasing for γ small enough. Moreover,*

$$\lim_{\gamma\to 0}\frac{\bar{c}(\gamma)^3}{\gamma^2} = \frac{1}{2}, \quad \textit{and} \quad \lim_{\gamma\to 0}\frac{\bar{c}(\gamma)}{\gamma} = +\infty.$$

Proof. Notice that the Lemma tells us that we need only show that the first term in (39) will be uniformly large when γ is small. Recall $q(\bar{c}) = 0$. If we multiply both sides of (21) by γ^2 and note that $\bar{c} \in (0, 1/2)$, it follows that

$$\lim_{\gamma \to 0} \bar{c}(\gamma) = 0.$$

From $q(\bar{c}) = 0$ it follows that

$$\lim_{\gamma \to 0} \left(\frac{2\bar{c}^3}{\gamma^2} + \bar{c}^2 + 2\bar{c} - 1 \right) = 0$$

and the first claim of the lemma follows. Since

$$\frac{\bar{c}}{\gamma} = \left(\frac{\bar{c}^3}{\gamma^2} \right)^{\frac{1}{3}} \frac{1}{\gamma^{\frac{1}{3}}}$$

the second limit follows as well. Using $q(\bar{c}) = 0$ we find that

$$\frac{d}{d\gamma} \frac{\bar{c}(\gamma)}{\gamma} = 4 \frac{\bar{c}^3}{\gamma^4} \left(\frac{6\bar{c}^2}{\gamma^2} + 2\bar{c} + 2 \right)^{-1} - \frac{\bar{c}}{\gamma^2}$$

Since $\bar{c}/\gamma \to +\infty$ as $\gamma \to 0^+$, it follows from this last that near $\gamma = 0$, the right hand side of this last equation is nearly $-\bar{c}/(3\gamma^2)$ and hence near $\gamma = 0$, $\frac{d}{d\gamma} \frac{\bar{c}(\gamma)}{\gamma} < 0$. □

If we can show that $e^{-\gamma^2 t}$ is bounded away from zero for γ small enough, then we can satisfy (39). We know that $T_{tr} \le t \le \alpha T_h$. We denote the dependence on γ by $T_{tr}(\gamma)$ and $T_h(\gamma)$. Using (32) we find

$$\begin{aligned} \gamma^2 T_{tr}(\gamma) &= -\frac{\gamma^2 \ln \varepsilon}{2\bar{c}(\gamma)} + \frac{\gamma^2 \ln Z(\gamma)}{2\bar{c}(\gamma)} \\ &= \frac{-\ln \varepsilon + \ln Z(\gamma)}{2} \left(\frac{\gamma^2}{\bar{c}^3} \right)^{\frac{1}{3}} \gamma^{\frac{4}{3}} \longrightarrow 0 \quad \text{for} \quad \gamma \to 0 \end{aligned}$$

and

$$\gamma^2 T_h(\gamma) = -\frac{\gamma^2 \ln \varepsilon}{2\bar{c}(\gamma)} \longrightarrow 0 \quad \text{for} \quad \gamma \to 0.$$

Hence we have shown the following:

Lemma 2.7. *There exists a $\gamma^*(\alpha) > 0$ such that for all $0 < \gamma < \gamma^*$ the inequality (39) is satisfied for all t with $T_{tr} \le t \le \alpha T_h$.*

From this Lemma and (37) we find that for all $x \in I_1$

$$u^+(x,t) \le 1 - \left(\frac{4}{\bar{c}} \vartheta \frac{\varepsilon e^{2\bar{c}t}}{1 - \varepsilon e^{2\bar{c}t}} \right).$$

We find

$$\frac{\varepsilon e^{2\bar{c}t}}{1 - \varepsilon e^{2\bar{c}t}} \longrightarrow \frac{\varepsilon^{1-\alpha}}{1 - \varepsilon^{1-\alpha}}, \quad \text{as} \quad t \to \alpha T_h.$$

Note that $\frac{\varepsilon^{1-\alpha}}{1-\varepsilon^{1-\alpha}}$ is a number independent of γ and $\bar{c}$. Since ϑ and $1/\bar{c}$ become large as $\gamma \to 0$, there is a $t^* > T_{tr}$, $t^* < \alpha T_h$ such that

$$u^+(x,t) < 0 \quad \text{for all} \quad x \in I_1,\ t^* \le t \le \alpha T_h,$$

which proves part (i) of the Theorem 2.3. Part (ii) follows by the same argument applied to u^-.

Moreover, for all $t \le \alpha T_h$ and for all $|x - \pi/2| < \kappa$ small enough and hence for all $x \in (\pi/2 - \delta, \pi/2 + \kappa)$ we get

$$1 + \left(4\bar{c} + \left(\frac{\pi}{2} - x\right) 4\gamma \frac{1-2\bar{c}}{\bar{c}} e^{-\gamma^2 t}\right) \frac{\varepsilon e^{2\bar{c}t}}{1 - \varepsilon e^{2\bar{c}t}} > 0,$$

which proves (iii) of the above Theorem 2.3. Again claim (iv) follows with a symmetrically used argument.

Finally, from the expansion of $u(x,t)$ as in Lemma 2.5 we see that

$$u(x,t) > 0, \quad \text{for all} \quad x \in (\pi/2 - \delta, \pi/2 + \delta),$$

which completes the proof of Theorem 2.3 □

3. Comparison results

In this section we first compare the blow-up results for the hyperbolic to the parabolic problem. Then we compare the three different choices of the turning rate $\mu^{\pm}$ as given in (3), (4) and (5). The last part of this section compares the third order operator which appears during the analysis of the hyperbolic system to the corresponding operator of the parabolic system. Indeed it turns out that the hodograph analysis, as done in [17] carries over without modification.

3.1. Comparison with the blow-up results in [17]

To compare the blow-up times of the unrestricted hyperbolic model (1) (3) with those of its parabolic limit (6), one must examine the characteristic equations which define the critical value $\bar{c}$. Here $\bar{c}$ is given as the smallest positive root of $q(c)$, where

$$q(c) = \frac{2}{\gamma^2} c^3 + c^2 + 2c - 1.$$

For $\gamma \to \infty$ the corresponding characteristic function for (6), is

$$q_{\text{LS}}(c) = c^2 + 2c - 1.$$

Its roots are $\sqrt{2} - 1$ and $-\sqrt{2} - 1$. Hence for (6), $\bar{c}_{\text{LS}} = \sqrt{2} - 1 \approx 0.41421$.

Thus,

$$q(\bar{c}_{\rm LS}) = \frac{2}{\gamma^2}(\sqrt{2}-1)^3 > 0$$

and for $c > \bar{c}_{\rm LS}$, one has $q_{\rm LS}(c) > 0$. Consequently, $q(c) > 0$ for all $c > \bar{c}_{\rm LS}$ and $0 < \bar{c} = \bar{c}(\gamma) < \bar{c}_{\rm LS}$ where $\bar{c}(\gamma)$ is the positive root of $q(c)$. Since $0 = 2(\bar{c})^3 + \gamma^2[(\bar{c})^2 + 2\bar{c} - 1]$ and since $\bar{c}(\gamma) \in (0,1)$ is a bounded function of γ it follows that

$$\lim_{\gamma\to+\infty} \bar{c}(\gamma) = \bar{c}_{LS} \tag{40}$$

and, as we saw above,

$$\lim_{\gamma\to+0} \bar{c}(\gamma) = 0. \tag{41}$$

Thus, in the limit of infinite mean particle speed, the blow up time approaches the parabolic blow up time while for zero particle speed, there is no blow up at all. That is, as the mean particle speed decreases to zero, the blow up time recedes to $+\infty$. In order to compare the blow-up times properly, we take the same initial data for the diffusion case as for the unrestricted hyperbolic case. The initial conditions for the diffusion based problem (6), are given in (7) and (8) whereas the initial conditions for the hyperbolic model are given by (30) with $v(x,0) = 0$. Observe that the initial data are different for $\bar{c} \neq \bar{c}_{\rm LS}$. For small ε, however, the difference is of order ε. We study $N = 2$ only.

For the moment, let ε and $\bar{c}_{\rm LS}$ refer to the diffusion based model of (6) and $\bar{\varepsilon}$ and $\bar{c}$ refer to the unrestricted hyperbolic model. The initial conditions for the signal W and S read

$$W(x,0) = \frac{1}{1+2\varepsilon\cos(2x)+\varepsilon^2} \qquad \text{and} \qquad S(x,0) = \frac{1}{1+2\bar{\varepsilon}\cos(2x)+\bar{\varepsilon}^2} \tag{42}$$

respectively. For ε and $\bar{\varepsilon}$ small enough, $W(x,0) \approx 1$ and $S(x,0) \approx 1$.

For the cell populations P and u, respectively,

$$P(x,0) \approx 1 - 4\varepsilon\bar{c}_{\rm LS}\cos(2x) \qquad \text{and} \qquad u(x,0) \approx 1 - 4\bar{\varepsilon}\bar{c}\cos(2x). \tag{43}$$

If

$$\bar{\varepsilon} := \varepsilon\frac{\bar{c}_{\rm LS}}{\bar{c}} \tag{44}$$

so that $\bar{\varepsilon} > \varepsilon$, then $|W(x,0) - S(x,0)| < c_1\varepsilon$ and $|P(x,0) - u(x,0)| < c_2\varepsilon$ for some constants c_1, c_2 independent of ε. Hence the data set for each problem converges uniformly to

$$[S,u](t=0) = [P,W](t=0) = [1,1]$$

as $\varepsilon \to 0$. The corresponding blow up time for the parabolic and unrestricted hyperbolic problems are given by:

$$T_p = \frac{-\ln\varepsilon}{2\bar{c}_{\rm LS}} \qquad \text{and} \qquad T_h = \frac{-\ln\bar{\varepsilon}}{2\bar{c}}.$$

respectively. A calculation gives

$$\frac{T_h}{T_p} = \frac{\bar{c}_{\rm LS}}{\bar{c}}\left[1 - \frac{1}{\ln \varepsilon}\ln\frac{\bar{c}_{\rm LS}}{\bar{c}}\right]. \tag{45}$$

Since $\bar{c}_{\rm LS} > \bar{c} > 0$ and $0 < \varepsilon < 1$ it follows that $T_h > T_p$. Both $T_h \to +\infty$ and $T_p \to +\infty$ as $\varepsilon \to 0^+$, as does their difference. However, we have:

Theorem 3.1. *Assume (P, W) and (u, S) are solutions of (6) and (1) respectively with initial values given in (42) and (43) with $\varepsilon, \bar{\varepsilon}$ related by (44). Then $T_h > T_p$ and*

$$\frac{T_h}{T_p} \to \frac{\bar{c}_{LS}}{\bar{c}}$$

from below as $\varepsilon \to 0^+$. Furthermore, this ratio approaches unity as $\gamma \to +\infty$, and $+\infty$ as $\gamma \to 0^+$ independent of ε.

Proof. This follows from (45), (40) and (41) since the latter two limits do not depend upon ε. □

Thus, although the data sets for each problem can be made arbitrarily close in the uniform norm, the blow up times will be arbitrarily far apart.

Now we compare the zero-turning-rate time T_{tr} of the hyperbolic problem to the parabolic blow-up time T_p.

Theorem 3.2. *Assume (P, W) and (u, S) are solutions of (6) and (1) respectively with initial values given in (42) and (43) with $\varepsilon, \bar{\varepsilon}$ related by (44). Then*

$$\frac{T_{tr}}{T_p} < \frac{\bar{c}_{LS}}{\bar{c}}.$$

Moreover we have

$$T_p < T_{tr} \qquad as \quad \varepsilon \to 0^+$$

and

$$T_p > T_{tr} \qquad as \quad \varepsilon \to 1^-.$$

Proof. The proof of this follows from the observation that

$$T_{tr} = \frac{\bar{c}_{\rm LS}}{\bar{c}}T_p - \frac{1}{2\bar{c}}\log\left[\frac{\bar{c}_{\rm LS}}{\bar{c}Z(\gamma)}\right]. \tag{46}$$

From the definition of $Z(\gamma)$ in (33) and the fact that $\bar{c}_{\rm LS} > \bar{c} > 0$, the argument of the logarithm is larger than unity. We use the explicit form of T_p to write the difference as

$$T_{tr} - T_p = \left(\frac{\bar{c}_{\rm LS}}{\bar{c}} - 1\right)\frac{\ln(1/\varepsilon)}{2\bar{c}_{\rm LS}} - \frac{1}{2\bar{c}}\log\left[\frac{\bar{c}_{\rm LS}}{\bar{c}Z(\gamma)}\right].$$

As $\varepsilon \to 0$ the first term on the right hand side dominates and is positive. As $\varepsilon \to 1$ the first term converges to zero and the negative second term dominates. Thus it is possible for the hyperbolic problem to develop vanishing turning rates before or after the parabolic problem blows up.

Example. In order to illustrate these blow-up times we choose the parameters according to a realistic example. For E. coli-bacteria as studied by Ford [6, **?**] we have a speed of $\gamma = 0.01\ \frac{\text{mm}}{\text{s}}$ and a diffusion constant of $D = 10^{-3}\ \frac{\text{mm}^2}{\text{s}}$. To make this clear: We do not claim that E. coli chemotaxis shows blow-up we just choose the above values get some numbers which we can compare explicitely. A realistic model for E. coli has to include saturation effects as will be discussed later.
In the foregoing analysis we nondimensionalized $D = 1$, hence we select a length scale of $\sqrt{10^{-3}}$ mm. In that scale $D = 1$ and $\gamma = 0.316$.
We know that $\bar{c}_{\text{LS}} = \sqrt{2} - 1$ and with use of MAPLE we find $\bar{c} = 0.26896$. We check two values for ε.
In case of $\varepsilon = 0.001$ we find

$$T_{tr} \approx 6.51 \text{ s}, \quad < \quad T_p \approx 8.34 \text{ s}, \quad < \quad T_h \approx 12.04 \text{ s}$$

and for $\varepsilon = 10^{-6}$ we get

$$T_p \approx 16.68 \text{ s}, \quad < \quad T_{tr} \approx 19.35 \text{ s}, \quad < \quad T_h \approx 24.88 \text{ s}.$$

Which shows that the blow-up time is about 50 % larger than in the comparable diffusion based model. In the first case $T_{tr} < T_p$ and in the latter case $T_{tr} > T_p$.

We saw in the previous example that the blow-up time depends sensitively on the size of γ. As the particle speed is decreased, the blow up time increases. In cases where $T_{tr} > T_p$ we find that the hyperbolic model is still a valid model (densities are positive) in a region where the diffusion based model already blows-up.

3.2. A local comparison result

In this section we show a result that implies that solutions to the exponential problem (system (1) with (5)) grow faster, and that solutions for the restricted problem (system (1) with (4)) grow slower than the blow-up solution of the unrestricted problem (system (1) with (3)). Before we do this we study system (1) for general $\mu^{\pm}$ first. As done above for the unrestricted problem, we transform system (1) into total particle density $u = u^+ + u^-$ and particle flux $v = u^+ - u^-$:

$$\begin{aligned} u_t + \gamma v_x &= 0 \\ v_t + \gamma u_x &= (\mu^- - \mu^+)u - (\mu^+ + \mu^-)v \\ S_t &= Su \end{aligned} \tag{47}$$

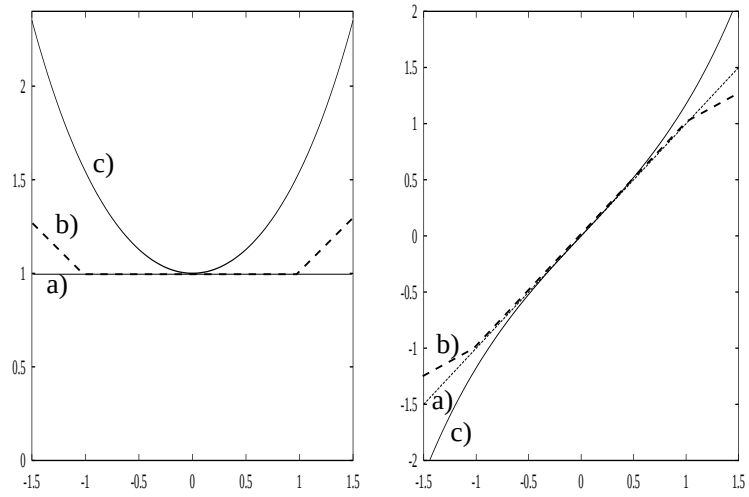

Figure 2. The right figure shows $\mu^+ + \mu^-$ and the left figure shows $\mu^- - \mu^+$ as functions of S_x for the three cases a), b), c), respectively.

The quantity $\mu^- - \mu^+$ is responsible for aggregation, whereas the term $\mu^+ + \mu^-$ in a sense, describes the adaptation/aggregation speed. We study these terms for the three cases a), b), c) which are relevant here.

In case a), (3), we have

$$\mu_a^- - \mu_a^+ = \frac{\gamma}{D}\chi(S)S_x, \qquad \mu_a^+ + \mu_a^- = \frac{\gamma^2}{D}. \tag{48}$$

For case b), (4), we find

$$\begin{aligned}
\mu_b^- - \mu_b^+ &= \begin{cases} -\frac{\gamma}{2D}(\gamma - \chi(S)S_x), & \text{if} \quad S_x < -\frac{\gamma}{\chi(S)} \\ \frac{\gamma}{D}\chi(S)S_x, & \text{if} \quad -\frac{\gamma}{\chi(S)} \le S_x \le \frac{\gamma}{\chi(S)} \\ \frac{\gamma}{2D}(\gamma + \chi(S)S_x), & \text{if} \quad \frac{\gamma}{\chi(S)} < S_x \end{cases} \\
\mu_b^+ + \mu_b^- &= \begin{cases} \frac{\gamma}{2D}(\gamma - \chi(S)S_x), & \text{if} \quad S_x < -\frac{\gamma}{\chi(S)} \\ \frac{\gamma^2}{D}, & \text{if} \quad -\frac{\gamma}{\chi(S)} \le S_x \le \frac{\gamma}{\chi(S)} \\ \frac{\gamma}{2D}(\gamma + \chi(S)S_x), & \text{if} \quad \frac{\gamma}{\chi(S)} < S_x \end{cases}
\end{aligned} \tag{49}$$

In case c), (5), we have

$$\mu_c^- - \mu_c^+ = \frac{\gamma^2}{D}\sinh\left(\frac{\chi(S)}{\gamma}S_x\right), \qquad \mu_c^+ + \mu_c^- = \frac{\gamma^2}{D}\cosh\left(\frac{\chi(S)}{\gamma}S_x\right). \tag{50}$$

For constant χ we sketch these six expressions in Figure 2.

We have

$$\mu_c^+ + \mu_c^- \ge \mu_b^+ + \mu_b^- \ge \mu_a^+ + \mu_a^- \ge 0 \tag{51}$$

and for $S_x < 0$ that

$$\mu_c^- - \mu_c^+ \le \mu_a^- - \mu_a^+ \le \mu_b^- - \mu_b^+ \le 0. \tag{52}$$

Now, to compare the unrestricted, the restricted and the exponential problem, we assume an initial condition with a single peak just a moment before the turning rates of the unrestricted problem would become negative somewhere. I.e. if $(u(x,t), v(x,t), S(x,t))$ denotes the solution of the unrestricted problem which we constructed above for $N = 2$ and $\varepsilon > 0$, then we choose initial conditions

$$(U_0(x), V_0(x), S_0(x)) := (u(x, T_{tr} - \nu), v(x, T_{tr} - \nu), S(x, T_{tr} - \nu)),$$

where T_{tr} is the zero turning rate time and $\nu > 0$ is small.

Theorem 3.3. *Let $(u_a, v_a, S_a), (u_b, v_b, S_b)$, and (u_c, v_c, S_c) denote the solutions of the unrestricted, restricted and exponential problem, respectively, with the same initial values (U_0, V_0, S_0). Then there exist $\delta > 0$ and a time $\tau > 0$ such that*

$$0 \le u_b(x,t) \le u_a(x,t) \le u_c(x,t) \tag{53}$$

for all $x \in (\pi/2 - \delta, \pi/2 + \delta)$ and $0 \le t < \tau$.

Proof. As in the previous section we expand the solution close to $\pi/2$ in terms of $(\pi/2 - x)$. We find that

$$u(x,t) \approx \alpha(t), \quad v(x,t) \approx (\pi/2 - x)\,\beta(t), \quad S_x(x,t) \approx (\pi/2 - x)\,\varphi(t), \tag{54}$$

with appropriate non-negative functions $\alpha(t), \beta(t), \varphi(t)$. If we use these expansions in (47) we find

$$\begin{aligned} \alpha_t &= \beta \\ \beta_t &= \tfrac{\mu^- - \mu^+}{\pi/2 - x}\alpha - (\mu^+ + \mu^-)\beta \\ \varphi_t &= \alpha\beta. \end{aligned} \tag{55}$$

We claim that for each of the cases a), b) and c) this system (with the corresponding $\mu^\pm$) describes the basic behavior near aggregation at $x = \pi/2$. For x close enough to $\pi/2$ the term which contains the difference $\mu^- - \mu^+$ dominates (as long as it is not zero). Hence we study

$$\begin{aligned} \alpha_t &= \beta \\ \beta_t &= \tfrac{\mu^- - \mu^+}{\pi/2 - x}\alpha \\ \varphi_t &= \alpha\beta. \end{aligned} \tag{56}$$

We solve the first equation of (56) to

$$\alpha(t) = \int_0^t \beta(s)ds.$$

For now we consider $x \ge \pi/2$ only. A symmetrically adapted argument applies for $x < \pi/2$. For $x \ge \pi/2$ we have $S_x \le 0$. Hence in any of the cases a), b),

and c) we find that

$$0 \leq \frac{\mu_b^- - \mu_b^+}{\pi/2 - x} \leq \frac{\mu_a^- - \mu_a^+}{\pi/2 - x} \leq \frac{\mu_c^- - \mu_c^+}{\pi/2 - x}$$

Hence, for the same chemical gradient $\varphi(t)$ the slope of the particle flux $\beta(t)$ grows fastest for β_c and slowest for β_b. If now β_a, β_b, and β_c is used in the third equation of (56) then we see that also

$$\varphi_b(t) \leq \varphi_a(t) \leq \varphi_c(t).$$

Hence the difference in the β's is enhanced. Finally, if

$$\beta_b(t) \leq \beta_a(t) \leq \beta_c(t),$$

then the same is true for α:

$$\alpha_b(t) \leq \alpha_a(t) \leq \alpha_c(t).$$

In (54) we restricted our attention to a small interval $(\pi/2 - \delta, \pi/2 + \delta)$. The higher order terms, which we neglected here, depend on time and they also grow as $t \to T_h$. Hence the expansion might not be valid for all times. □

3.3. Dissipative third-order operators and the pseudo-hodograph plane.

In [17] a pseudo hodograph-plane analysis for the second order operator $\Psi \mapsto \Psi_{tt} + a(\Psi_x \Psi_t)_x$ was used to identify hyperbolic, parabolic and elliptic regions in a (Ψ_x, Ψ_t) - plane. The region in the (x,t) plane for which $\Psi_x^2 - 4\Psi_t < 0$ was designated as the elliptic region while the region for which $\Psi_x^2 - 4\Psi_t > 0$ was designated as the hyperbolic region.

The third order operator

$$Q_{\text{LS}}\Psi = \Psi_{txx}$$

which is strongly damping, was neglected for that argument in order to better understand the hyperbolic character of the operator.
In the case studied here, the corresponding third order operator is (see (16))

$$Q_h\Psi := \Psi_{txx} - \frac{1}{\gamma^2}\Psi_{ttt}.$$

Using the Fourier-transform, one can see that Q_h is also dissipative and strongly damping. To see this, consider the equation

$$\varphi_{tt} = Q_h\varphi$$

and look for solutions of the form $\varphi = \exp(\lambda t + ikx)$. The dispersion relation for Q_{LS} reads $\lambda_{LS}(k) = -k^2$ for the modes $k \in \mathbb{N}$, which is strongly damping away from $k = 0$. The eigenvalue $\lambda = 0$ for $k = 0$ corresponds to the conservation of

particle property of the underlying system (6).
In our case, $\lambda_h = 0$ or

$$\lambda_h^{\pm}(k) = -\frac{\gamma^2}{2} \pm \frac{\gamma^2}{2}\sqrt{1 - \frac{4k^2}{\gamma^2}}.$$

Thus $\lambda_h^{\pm}(k)$ is either negative or has negative real part according as $\frac{k}{\gamma} \leq \frac{1}{2}$ or $\frac{k}{\gamma} > \frac{1}{2}$. Hence Q_h can be viewed as strongly damping.

The whole hodograph-analysis of [17] therefore carries over to this case when the side requirement of the positivity of the turning rates is set aside. Then the blow-up mechanism is the same in both equations, although the blow-up times can be quite different.

In particular, for the exact solution of (6) given above, it was found that the blow up point occurred on the parabolic boundary of these two regions precisely at $x = \pi/2$ and that the initial data satisfied $\Psi_x^2(x,0) - 4\Psi_t(x,0) < 0$ (as did the initial data in [22]) when $|\varepsilon| << 1$.

Similarly, in the situation here, the initial values satisfy the same ellipticity condition in spite of the fact that the turning rates are initially positive. Furthermore, the example shows that the sign of the turning rates change when $|\Psi_x| = \gamma$ while the blow up of the solution occurs on the boundary of the region where $\Psi_x^2 > 4\Psi_t$. This means that the turning rates become negative on the parabolic boundary near the blow-up point and that the curve along which the turning rates vanish is contained in that part of the hyperbolic region where $\Psi_x^2 = \gamma^2 > 4\Psi_t$.

Notice, however, that along the line $x = \pi/2$, both turning rates are positive, indeed constant, until the moment of blow up. Thus a "shock" is forming in the turning rates at the blow up time.

4. Relevance of the blow-up models to biology

Models such as those given in (1) or (6) with a rate law $R(X,Y) = XY$ and a chemotactic sensitivity $\chi(X) = 1/X$ lead to solutions which blow up in finite time and therefore cannot be biologically realistic. However, these choices are limiting cases of more realistic forms of the rate law and the sensitivity. For example, a more realistic choice for the rate law (where Y is thought of as the particle density while X is the chemical concentration) is

$$R(X,Y) = \frac{K_{cat}XY}{K_m + X} \tag{57}$$

which indicates that a type of Michealis-Menten enzyme kinetic hypothesis underlies the chemistry involved in the particle response to the chemical. The constants $(K_{cat}, K_m$ have their usual meaning. See Murray [19].) Clearly, our choice $R(X,Y) = XY$ corresponds to the limiting case of very low chemical concentration X. Likewise, the choice $\chi(X) = 1/X$ corresponds to the statement that the particles are "infinitely" sensitive to X even at "infinite dilution." This too is not biologically realistic and must be replaced by a more reasonable hypothesis. For example, one might assume, following, [22] that the particles are relatively insensitive to large concentrations of the chemical but are moderately sensitive to very low concentrations of the chemical. This would lead to

$$\chi(X) = \frac{1}{(a+X)(b+X)}, \quad \text{where} \quad 0 < a << 1 << b. \tag{58}$$

The numerical observations of [22] for (6) with these choices and the corresponding theoretical rationale for them given in [17] confirm that the choices of (57), (58) preclude blow up in finite time. Roughly, the reason for this is as follows. Associated with the system (6) there is a quasi-linear second order operator $\mathcal{L}\psi = \psi_{tt} + A(\psi_x, \psi_t)\psi_{xt} + B(\psi_x, \psi_t)\psi_{xx}$ which, for small values of the chemical $X = W$, is elliptic. When the initial data is such that the evolution starts in the elliptic region (as it does for small perturbations of a uniform particle distribution and small chemical concentration), the problem is ill posed and the solution components of the vector $(Y, X) = (P, W)$ attempt to blow up in finite time. As this occurs, the approximation to $R(X,Y)$ as the product XY and of $\chi(X)$ to $1/X$ are no longer appropriate. In the regime in which we have saturation, $\mathcal{L}$ becomes hyperbolic. This change in type together with any damping terms present, is responsible for the solution to have a "change of heart", abandon its attempt to form singularities and collapse. However the collapse cannot be complete since regions have formed in the (x,t) plane whose boundaries are caustics that prohibit the transport of particles from the blow up region completely back to a constant steady state. The aggregation of particles into a (nearly) piecewise constant distribution then results.

The numerical simulations we give below for (1) with these more biologically reasonable choices for R, χ, (57), (58), show precisely the same behavior. This can be seen quite clearly in Figures 3, 4, and 5. As the initial chemical concentration falls, the particle density tends to form a singularity (compare the vertical scales in the first of Figure 3 and in Figure 5).

4.1. Numerical simulations

We present simulations for (1) on an interval $I = [0,1]$ with homogeneous Neumann boundary conditions (2). The parameter functions are chosen according to the simulations of Othmer and Stevens [22] and Levine and Sleeman [17] for the related diffusion based model (6). This permits us to compare the results pre-

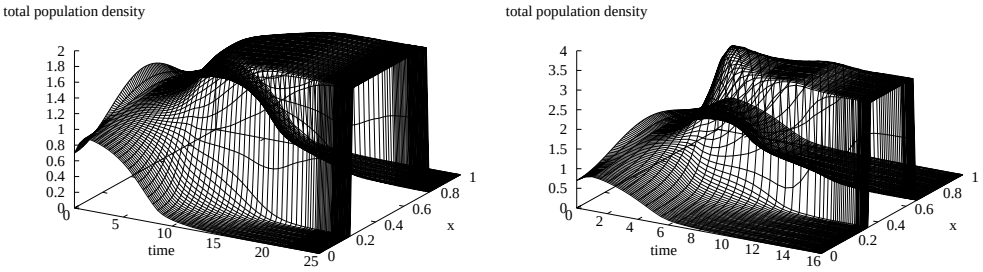

Figure 3. Evolution of the cell density for different values of S_0 . left: $S_0 = 1000$, right: $S_0 = 100$. The other parameters are as shown in the text.

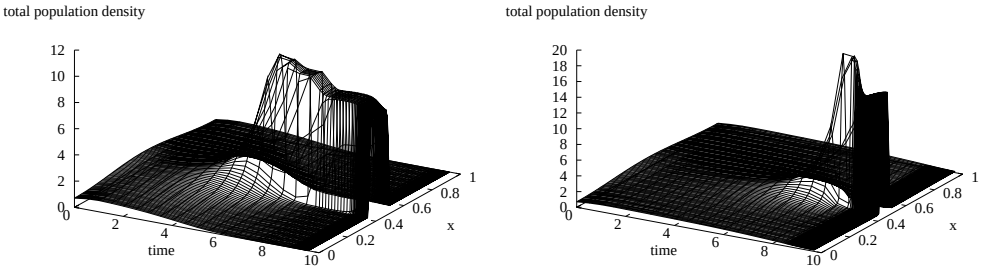

Figure 4. Evolution of the cell density for different values of S_0 . left: $S_0 = 1$, right: $S_0 = 0.01$. The other parameters are as shown in the text.

sented here to the patterns found in [22] and [17].
In the following situations we used a *chemotactic sensitivity* of

$$\chi(S) = \frac{D\delta}{(\gamma + S)(\beta + S)} \quad \text{with} \quad \delta = 1000, \gamma = 1000, \beta = 0.01.$$

The turning rates $\mu^{\pm}$ are given in the restricted form by (4), with particle speed $\gamma = 0.5$ and "effective" diffusion constant $D = 0.04$.
The production function for S is chosen as

$$R(S, u^+ + u^-) = -\mu S + \frac{\lambda S(u^+ + u^-)}{1 + \nu S},$$

with $\nu = 0.00001$ and $\mu = 1$. Levine and Sleeman used a decay rate of $\mu = 10$ but this rate appears to be too strong for the model presented here. In all

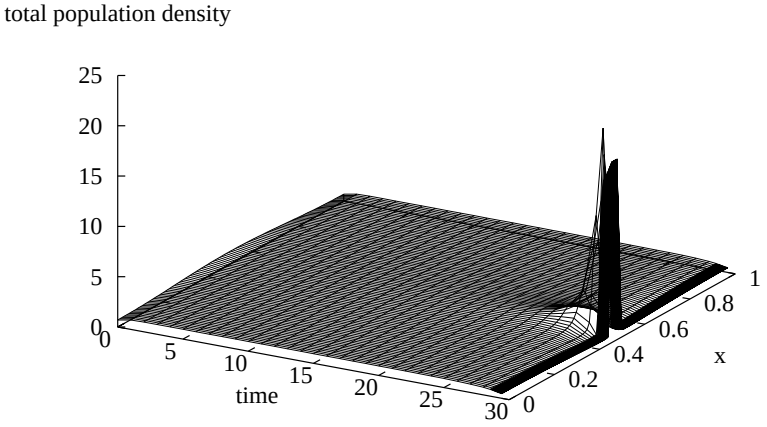

Figure 5. Evolution of the cell density for $S_0 = 0.001$. The other parameters are as shown in the text.

simulations it led to collapse. The initial conditions are

$$\begin{aligned} u^+(0,x) &= 0.5 - 0.15\cos(2\pi x), \\ u^-(0,x) &= 0.5 - 0.15\cos(2\pi x), \\ S(0,x) &= S_0, \end{aligned}$$

with a constant S_0 to be specified later.

We use a conservative Godunov scheme, which preserves the total particle density. We impose time step adaptation. If the local gradient becomes too steep then the numerical solution can become negative. If this happens we reduce the time step by a factor 0.5 and re-calculate the last iterate. The spatial discretization is $dx = 0.01$ and the time step size is adjusted to the particle speed, γ, as to meet the CFL-condition. We chose

$$dt = 0.1\frac{dx}{2\gamma}.$$

We carefully checked that the dynamic behavior, as presented below, does not depend on the choice of time and space discretizations (as long as they are reasonable).

The following series of simulations, Figures 3 - 5, illustrates the dynamic behavior with decreasing initial condition for S:

References

[1] A. R. A. Anderson and M. A. J. Chaplain, Modelling the growth and form of capillary networks. In J. C. McLachlan M. A. J. Chaplain, G. G. Singh, editor, *On Growth and Form: Spatio-Temporal Pattern formation in Biology*, Wiley, 1999, 225–249.

[2] A. R. A. Anderson and M. A. J. Chaplain, A mathematical model for capillary network formation in the absence of endothelial cell proliferation. *Appl. Math. Lett.* **11** (1998), 109–116.

[3] Y. Dolak and T. Hillen, Cattaneo models for chemotaxis, numerical solution and pattern formation. *J. Math. Biol.* **46**(2) (2003), 153–170.

[4] A. Einstein, Zur Theorie der Brownschen Bewegung. *Annalen der Physik* **19** (1906), 371–381.

[5] R. M. Ford and D. A. Lauffenburger, Measurement of bacterial random motility and chemotaxis coefficients: II. application of single cell based mathematical model. *Biotechnol. Bioeng.* **37** (1991), 661–672.

[6] R. M. Ford, B. R. Phillips, J. A. Quinn and D. A. Lauffenburger, Measurement of bacterial random motility and chemotaxis coefficients: I. stopped-flow diffusion chamber assay. *Biotechnol. Bioeng.* **37** (1991), 647–660.

[7] T. Hillen, Hyperbolic models for chemosensitive movement. *Math. Models Methods Appl. Sci.* **12**(7) (2002), 1007–1034.

[8] T. Hillen and H. G. Othmer, The diffusion limit of transport equations derived from velocity jump processes. *SIAM J. Appl. Math.* **61**(3) (2000), 751–775.

[9] T. Hillen, C. Rohde, and F. Lutscher, Existence of weak solutions for a hyperbolic model for chemosensitive movement. *J. Math. Anal. Appl.* **260** (2001), 173–199.

[10] T. Hillen and A. Stevens, Hyperbolic models for chemotaxis in 1-d. *Nonlinear Analysis: Real World Applications* **1**(1) (2001), 409–433.

[11] W. Jäger and S. Luckhaus, On explosions of solutions to a system of partial differential equations modelling chemotaxis. *Trans. AMS* **329** (1992), 819–824.

[12] E. F. Keller and L. A. Segel, Initiation of slime mold aggregation viewed as an instability. *J. Theor. Biology* **26** (1970), 399–415.

[13] H. A. Levine, S. Pamuk, B. D. Sleeman, and M. Nilsen-Hamilton, Mathematical modeling of capillary formation and development in tumor angiogenesis: Penetration into the stroma. *Bull. Math. Biol.* (2001), 801–863.

[14] H. A. Levine and B. D. Sleeman, A system of reaction diffusion equations arising in the theory of reinforced random walks. *SIAM J. Appl. Math.* (1997), 683–730.

[15] H. A. Levine, B. D. Sleeman, and M. Nilsen-Hamilton, A mathematical model for the roles of pericytes and macrophages in the onset of angiogenesis: I. the role of protease inhibitors in preventing angiogenesis. *Math. Biosci.* (2000), 77–115.

[16] H. A. Levine, B. D. Sleeman, and M. Nilsen-Hamilton, Mathematical modeling of the onset of capillary formation initiating angiogenesis. *J. Math. Biol.* (2001), 195–238.

[17] H. A. Levine and B. D. Sleeman, A system of reaction diffusion equations arising in the theory of reinforced random walks. *SIAM J. Appl. Math.* **57** (1997), 683–730.

[18] F. Lutscher, Modeling alignment and movement of animals and cells. *J. Math. Biol.* **45** (2002), 234–260.

[19] J. D. Murray, *Mathematical Biology*. Springer, 1989.

[20] H. G. Othmer and T. Hillen, The diffusion limit of transport equations (ii): Chemotaxis equations. *SIAM J. Appl. Math.* **62**(4) (2002), 1122–1250.

[21] H. G. Othmer and P. Schaap, Oscillatory cAMP signaling in the development of dictyostelium discoideum. *Comm. Theor. Biol.* **89** (1990), 510 – 517.

[22] H. G. Othmer and A. Stevens, Aggregation, blowup and collapse: The ABC's of taxis in reinforced random walks. *SIAM J. Appl. Math.* **57** (1997), 1044–1081.

[23] C. S. Patlak, Random walk with persistence and external bias. *Bull. Math. Biophys.* **15** (1953), 311–338.

[24] M. A. Rivero, R. T. Tranquillo, H. M. Buettner, and D. A. Lauffenburger, Transport models for chemotactic cell populations based on individualcell behavior. *Chem. Eng. Sci.* **44** (1989).
[25] L. A. Segel, A theoretical study of receptor mechanisms in bacterial chemotaxis. *SIAM J. Appl. Math.* **32** (1997), 653–665.
[26] D. D. Woodward, R. Tyson, M. R. Myerscough, J. D. Murray, E. Budrene, and H. C. Berg, Spatio-temporal patterns generated by *Salmonella typhimurium*. *Biophys. J.* **68** (1995), 2181–2189.

T. Hillen
University of Alberta
Edmonton T6G 2G1
Canada
e-mail: thillen@ualberta.ca

H. A. Levine
Iowa State University
Ames, Iowa 50011
U.S.A.
e-mail: halevine@iastate.edu

(Received:)